J|A|C|S
ARTICLES
Published on Web 12/11/2003

The Role of Intermolecular and Molecule−Substrate Interactions in the Stability of Alkanethiol Nonsaturated Phases on Au(111)

Esther Barrena,*[,†,#] Elisa Palacios-Lidón,[†] Carmen Munuera,[†] Xavier Torrelles,[‡] Salvador Ferrer,[§] Ulrich Jonas,[||] Miquel Salmeron,[⊥] and Carmen Ocal[†]

Contribution from the Instituto de Ciencia de Materiales de Madrid, Consejo Superior de Investigaciones Científicas (CSIC) Cantoblanco, 28049 Madrid, Spain, Institut de Ciència des Materials de Barcelona (CSIC), Campus de la Universitat Autònoma de Barcelona, 08193 Bellaterra, Spain, European Synchrotron Radiation Facility, BP 220, 38043 Grenoble Cedex, France, Max-Planck-Institute for Polymer Research, Ackermannweg 10, D-55128 Mainz, Germany, and Lawrence Berkeley National Laboratory, University of California, Berkeley, California 9470

Received May 14, 2003; E-mail: barrena@mf.mpg.de

Abstract: The structure and stability of alkanethiols self-assembled on Au(111) have been studied as a function of the molecular chain length by means of atomic force microscopy (AFM) and grazing incidence X-ray diffraction (GIXD). Below saturation, phases consisting of molecules with different tilt angles and periodicities are formed. Differences in the mechanical stability of these phases are revealed by AFM experiments and discussed in terms of the competition between intermolecular and molecule−substrate interactions as a function of chain length. For long molecules, intermolecular interactions play a dominant role which stabilizes the formation of closed packed 30° tilted ($\sqrt{3}\times\sqrt{3}$)R30° structures. For short molecules, the van der Waals interaction with the gold substrate favors the formation of a 50° tilted phase in which the molecules are arranged in a rectangular configuration.

1. Introduction

The potential application of self-assembled monolayers (SAM) in different fields of science and technology has motivated a large number of studies in recent years.[1] It has become clear that the design of films with specific controlled properties requires a better understanding of the parameters governing the self-assembly process. Alkanethiols ($SH-(CH_2)_{n-1}-CH_3$, referred to as C*n* from now on) on Au(111) possess two important characteristics: structural simplicity and well-defined order, which make them ideal for understanding the role that the fundamental interactions play in determining the self-assembled structure. Thus, beyond their technological interest, they are considered model systems for SAM. Enormous effort has been devoted to studying the structure and kinetics of the SAM formation. For an excellent overview and state of the art, see the review by Schreiber.[1] Self-assembling can be obtained either from vapor phase deposition in ultrahigh vacuum (UHV) or from solution, and, among the different phases reported, it is well established that the lowest energy phase for full-coverage films consists of molecules ordered in a close-packed ($\sqrt{3}\times\sqrt{3}$)R30° lattice modulated by a $c(4\times 2)$ superstructure.[1−6] The close-packed structure, commensurate with the gold substrate, has a lattice parameter of 4.99 Å (distance between next-nearest Au(111) neighbors).[7−11] Because the diameter of the alkane chains is around 4.3 Å, that is, 0.7 Å smaller than the separation between their headgroups, the molecules tilt (∼30−35° from the surface normal) so that the distance between chains approaches this value, thus optimizing the intermolecular van der Waals interaction.

For a wide range of coverage below the monolayer completion, different ordered molecular structures appear. Particular attention has been devoted in the literature to phases where molecules are arranged forming stripes on the surface, the so-called "striped phases", which have been observed by different techniques.[12−28]

[†] Consejo Superior de Investigaciones Científicas (CSIC) Cantoblanco.
[‡] Campus de la Universitat Autònoma de Barcelona.
[§] European Synchrotron Radiation Facility.
[||] Max-Planck-Institute for Polymer Research.
[⊥] Lawrence Berkeley National Laboratory.
[#] Current address: Max-Planck-Institut für Metallforschung, Heisenbergstrasse 3, 70569 Stuttgart, Germany.

(1) Schreiber, F. *Prog. Surf. Sci*. **2000**, *65*, 151−256.
(2) Camillone, N., III; Chidsey, C. E. D.; Liu, G.; Scoles, G. *J. Chem. Phys.* **1993**, *98*, 3503−3511.
(3) Fenter, P.; Eisenberger, P.; Liang, K. S. *Phys. Rev. Lett.* **1993**, *70*, 2447−2450.
(4) Poirier, G. E.; Tarlov, M. J. *Langmuir* **1994**, *10*, 2853−2856.
(5) Delamarche, E.; Michel, G.; Gerber, C.; Anselmetti, D.; Güntherodt, H.-J.; Wolf, H.; Ringsdor, H. *Langmuir* **1994**, *10*, 2869−2871.
(6) Fenter, P.; Eberhardt, P.; Eisenberger, P. *Science* **1994**, *266*, 1216−1218.
(7) Strong, L.; Whitesides, G. M. *Langmuir* **1988**, *4*, 546−558.
(8) Chidsey, C. E. D.; Liu, G.-Y.; Rowntree, P.; Scoles, G. *J. Chem. Phys*. **1989**, *91*, 4421−4423.
(9) Ulman, A.; Eilers, J. E.; Tillman, N. *Langmuir* **1989**, *5*, 1147−1152.
(10) Nuzzo, R. G.; Dubois, L. H.; Allara, D. L. *J. Am. Chem. Soc.* **1990**, *112*, 558−569.
(11) Widrig, C. A.; Alves, C. A.; Porter, M. D. *J. Am. Chem. Soc*. **1991**, *113*, 2805−2810.

The lowest density striped phase consists of rows of fully stretched molecules parallel to the surface with a distance between rows which is approximately twice the length of the molecule. The stripes run along the next-nearest-neighbor (NNN) direction of Au(111) with a periodicity of 5 Å along the row. Increasing coverage leads to the formation of denser striped phases with a lower distance between rows.[20,21,25] The striped phases have been generally denoted by $p\times\sqrt{3}$, where the corresponding $\sqrt{3}$ and p indicate the periodicities along and between stripes, respectively, in terms of the Au(111) nearest-neighbor distance (NN). Some of these phases have been also obtained by annealing from the denser $(\sqrt{3}\times\sqrt{3})$R30° monolayer.[14,15,17,22,26] Although most characterization has been obtained from gas-phase deposition studies,[12,14−17,21,23,25] identical striped structures have been also obtained at low coverage deposited from solution.[20,29]

Whereas the structures of the lowest density striped phases and the full-coverage phase are well characterized, the picture at intermediate coverage is rather complex and has been mostly studied for short molecules ($n \leq 10$).[12,13,8,21,30−34] In particular, Poirier and co-workers have extensively studied the structural phases of decanethiol molecules (C10) on Au(111)[16,25,27] prepared under UHV conditions from vapor deposition. A phase diagram of C10 on Au(111), in temperature and coverage space, has been obtained by GIXD[23] and STM.[35]

Many other structures at intermediate coverage have been reported for alkanethiols on Au(111),[12,13,32−34,36−38] leading to lack of agreement sometimes in the literature. Some of these phases have been either grown (from solution or in UHV) or obtained by annealing from the denser $(\sqrt{3}\times\sqrt{3})$R30° monolayer and ascribed to upright configurations.[12,28,32,36−39] It is likely that, at intermediate coverage, a broad spectrum of different nonequilibrium structures, and coexistence between them, would be achieved depending on preparation conditions and chain length.[1,40] However, many structural studies do not provide direct information about the molecular density nor about film height, making it difficult to determine the number of molecules per unit cell and the true molecular configuration (flat, tilted, or upright molecules).

Until now, most evidence for intermediate structures has been obtained from scanning tunneling microscopy (STM), which does not provide information for chains longer than 12 carbons due to the large gap resistance of these films. However, because GIXD studies on monolayers with $10 \leq n \leq 20$ have revealed some deviations of tilt and azimuthal angles at $n < 14$,[41] we believe that also for intermediate coverage phases, consisting of nearly standing upright molecules, structural differences would exist between short and long molecules. These differences can be rather important due to the balance between competing interactions.

A recent AFM study of low coverage films of octadecanethiol (C18) prepared on Au(111) from solution has shown the existence of a commensurate $(2\times\sqrt{3})$ rectangular structure.[42] The area per molecule is ∼29 Å^2 (in the $c(4\times2)$, this area is ∼21.6 Å^2), and the molecules are tilted ∼50° from the surface normal. This structure as well as other tilted configurations arise from the optimization of the van der Waals energy of the molecular packing (interlocking of the chains) while keeping the criteria of commensurability to optimize the energy of the interface. This rectangular phase was shown to be metastable because after perturbation by increasing the load of the scanning AFM tip, the molecules rearrange in the lowest energy $(\sqrt{3}\times\sqrt{3})$R30° structure.

On the basis of this observation, we have investigated whether similar tilted phases exist for other alkanethiol molecules (C22, C18, and C10) and how their stability depends on chain length. The study has been performed using contact-mode AFM in ambient conditions. By carefully controlling the applied force, we could obtain an accurate measurement of the molecular lattice periodicity as well as the film height without inducing damage. Control of the applied force also permitted intentional damage of the structures to test their stability. In addition to the AFM experiments, some GIXD measurements have been used to support structural determination of the observed phases.

The present study shows for the first time the formation of ordered 50° tilted configurations at intermediate coverage (between that of the striped phases and the close-packed monolayer) and for molecules of different chain lengths. Important differences are found for the shortest chain, in terms of both structure and stability.

Even though the covalent S−Au interaction is dominant in the monolayer formation and assembly, the stability of the films also depends on the balance of other contributions including intermolecular or chain−chain interactions and molecule−substrate interactions.

(12) Dubois, L. H.; Zegarski, B. R.; Nuzzo, R. G. J. *J. Chem. Phys.* **1993**, *98*, 678−688.
(13) Poirier, G. E.; Tarlov, M. J.; Rushmeier, H. E. *Langmuir* **1994**, *10*, 3383−3386.
(14) Camillone, N., III; Eisenberger, P.; Leung, T. Y. B.; Schwartz, P.; Scoles, G.; Poirier, G. E.; Tarlov, M. J. *J. Chem. Phys.* **1994**, *101*, 11031−11036.
(15) Camillone, N., III; Leung, T. Y. B.; Schwartz, P.; Eisenberger, P.; Scoles, G. *Langmuir* **1996**, *12*, 2737−2746.
(16) Poirier, G. E.; Pyland, E. D. *Science* **1996**, *272*, 1145−1148.
(17) Gerlach, R.; Polanski, G.; Rubahn, H.-G. *Appl. Phys. A* **1997**, *65*, 375−377.
(18) Himmel, H.-J.; Wöll, Ch.; Gerlach, R.; Polankski, G.; Rubahn, H.-G. *Langmuir* **1997**, *13*, 602−605.
(19) Voets, T.; Gerritsen, J. W.; Grimbergen, R. F. P.; van Kempen, H. *Surf. Sci.* **1998**, *399*, 316−323.
(20) Yamada, R.; Uosaki, K. *Langmuir* **1998**, *14*, 855−861.
(21) Kondoh, H.; Kodama, C.; Sumida, H.; Nozoye, H. *J. Chem. Phys.* **1999**, *111*, 1175−1184.
(22) Staub, R.; Toerker, M.; Fritz, T.; Schmitz-Hübsch, T.; Sellan, F.; Leo, K. *Langmuir* **1998**, *14*, 6693−6698.
(23) Schreiber, F.; Eberhardt, A.; Leung, T. Y. B.; Schwartz, P.; Wetterer, S. M.; Lavrich, D. J.; Berman, L.; Fenter, P.; Eisenberger, P.; Scoles, G. *Phys. Rev. B* **1998**, *57*, 12476−12481.
(24) Xu, S.; Cruchon-Dupeyrat, S.; Garno, J. C.; Liu, G.-Y.; Jennings, G. K.; Yong, T.-H.; Laibnis, P. E. *J. Phys. Chem. B* **1998**, *102*, 5002−5012.
(25) Poirier, G. *Langmuir* **1999**, *15*, 1167−1175.
(26) Toerker, M.; Staub, R.; Fritz, T.; Schmitz-Hübsch, T.; Sellan, F.; Leo, K. *Surf. Sci*. **2000**, 445, 100−108.
(27) Fitts, W. P.; White, J. M.; Poirier, G. E. *Langmuir* **2002**, *18*, 1561−1566.
(28) Qian, Y.; Yang, G.; Yu, J.; Jung, T. A.; Liu, G.-Y. *Langmuir* **2003**, *19*, 6056−6065.
(29) Yamada, R.; Uosaki, K. *Langmuir* **1997**, *13*, 5218−5221.
(30) Porter, M. D.; Bright, T. B.; Allara, D. L.; Chidsey, C. E. D. *J. Am. Chem. Soc.* **1987**, *109*, 3559−3568.
(31) Alves, C. A.; Smith, E. L.; Porter, M. D. *J. Am. Chem. Soc*. **1992**, *114*, 1222−1227.
(32) Kang, J.; Rowntree, P. A. *Langmuir* **1996**, *12*, 2813−2819.
(33) Noh, J.; Hara, M. *Langmuir* **2002**, *18*, 7280−7285.
(34) Noh, J.; Hara, M. *Langmuir* **2002**, *18*, 1953−1956.
(35) Poirier, G. E.; Fitts, W. P.; White, J. M. *Langmuir* **2001**, *17*, 1176−1183.
(36) Schönenberger, C.; Jorritsma, J.; Sondag-Huethorst, J. A. M.; Fokkink, L. G. J. *J. Phys. Chem.* **1995**, *99*, 3259−3271.
(37) Gerlach, R.; Polanski, G.; Rubahn, H.-G. *Thin Solid Films* **1998**, *318*, 270−272.
(38) Xiao, W.; Wang, B.; Zhang, C.; Yang, Z.; Loy, M. M. T. *Surf. Sci.* **2001**, *472(1−2)*, 41−50.
(39) Truong, K. D.; Rowntree, P. A. *J. Phys. Chem.* **1996**, *100*, 19917−19926.
(40) Schwartz, D. K. *Annu. Rev. Phys. Chem.* **2001**, *52*, 107−137.
(41) Fenter, P.; Eberhardt, A.; Liang, K. S.; Eisenberger, P. *J. Chem. Phys.* **1997**, *106*, 1600−1608.
(42) Barrena, E.; Ocal, C.; Salmeron, M. *J. Chem. Phys.* **2001**, *114*, 4210−4214.

To estimate the difference in energy between the 50° and the 30° tilted configurations as a function of the chain length, we have developed a simple model, which is used to discuss the results and provide an understanding of the role of the competing interactions in the energetic balance of the self-assembly process.

2. Experimental Section

Alkanethiol chains $C_{18}H_{37}SH$ (C18) and $C_{10}H_{21}SH$ (C10) from Aldrich were used as received. $C_{22}H_{45}SH$ (C22) was synthesized starting from 1-bromodocosane ($C_{22}H_{45}Br$), as specified below. Gold substrates were purchased from Metallhandel Schröer GmbH (200−300 nm of gold over 1−4 nm of chromium on glass) and prepared by flame-annealing in air after cleaning in a piranha solution (1:3; H_2O_2:H_2SO_4). The resulting surface consisted of large grains with flat terraces of (111) orientation (sizes up to 400 nm) separated by monatomic steps. Flatness and cleanness were tested by the quality of the lattice-resolved images of the gold substrate. For GIXD studies, a gold single crystal with a miscut angle < 0.25° off the (111) orientation (MaTeck) was used. The Au(111) substrate was cleaned by repeated argon-ion bombardment and annealing cycles. Surface structure and cleanness were verified by Auger electron spectroscopy (AES), low energy electron diffraction (LEED), and AFM.

The samples were prepared at room temperature (~21 °C) by immersing the gold substrates in 0.2 μM solutions of C*n* in ethanol for time periods of 10−50 s. After this, they were rinsed with absolute ethanol and dried under an N_2 stream. This procedure led to the formation of alkylthiol islands with various sizes and morphologies. As reported before,[43] the molecular order of the islands improves with storage time in ambient conditions. The AFM images shown here were acquired 24 h after the preparation.

AFM measurements were performed under ambient conditions with a homemade microscope head,[44] combined with an SPM100 control unit and software from Nanotec. We used V-shaped Si_3N_4 sharpened cantilevers with nominal force constants of $K = 0.10$ N/m (Park Scientific Instruments) and rectangular cantilevers with $K = 0.37$ N/m (Olympus). Force versus distance curves were systematically obtained to check tip conditions by measurement of the adhesion force.

The GIXD measurements were performed in a UHV chamber mounted on a six-circle diffractometer at the ID03 beamline of the European Synchrotron Radiation Facility (ESRF). The X-ray energy was fixed at 16.98 keV (0.73 Å), and the measurements were performed at the critical angle (0.26°).

Synthesis of Docosane-1-thiol ($C_{22}H_{45}SH$): 1-Bromodocosane ($C_{22}H_{45}Br$, 3 g, 7.7 mmol, from ABCR, Germany) was refluxed in 50 mL of ethanol, 7.64 g (30.8 mmol) of sodium thiosulfate (pentahydrate) in 80 mL of H_2O was added and refluxed for 3 h, and then the same amount of sodium thiosulfate was added and refluxed for 3 days. After the mixture was cooled to room temperature, sodium *S*-docosyl thiosulfate ($C_{22}H_{45}S_2O_3Na$) precipitated and was recrystallized in ethanol to yield 2.03 g (4.6 mmol, 60% o. th., mp 126 °C). ^{1}H NMR (250 MHz, $CDCl_3$): δ (ppm) 0.88 (t, $J = 7.5$ Hz, 3H, $-CH_3$), 1.2−1.3 (br m, 36H, $-CH_2-$), 1.47 (br s, 2H, γ-CH_2-), 1.67 (m, $J = 7.5$ Hz, 2H, β-CH_2-), 2.68 (t, $J = 7.5$ Hz, 2H, α-CH_2-). The sodium *S*-docosyl thiosulfate (1 g, 2.25 mmol) was refluxed under nitrogen atmosphere in 25 mL of concentrated HCl for 2 h. After the mixture was cooled, the crude docosane-1-thiol precipitated and was vacuum distilled (kugelrohr, 2×10^{-2} Torr, 250 °C) to yield 0.67 g (2 mmol, 87% o. th.) of pure thiol. ^{1}H NMR (250 MHz, $CDCl_3$): δ (ppm) 0.88 (t, $J =$ 7.5 Hz, 3H, $-CH_3$), 1.2−1.4 (br m, 38H, $-CH_2-$), 1.61 (m, $J = 7.5$ Hz, 2H, β-CH_2-), 2.52 (q, $J = 7.5$ Hz, 2H, α-CH_2-). MS (EI) calcd for $C_{22}H_{46}S$ [M^+] *m*/*z* 342.67, found 342.

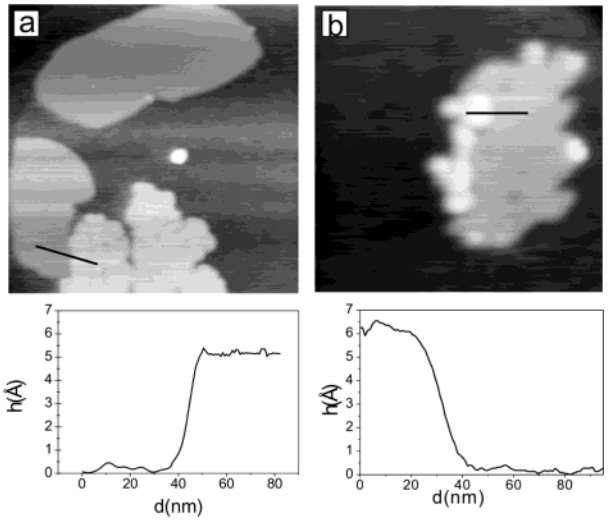

Figure 1. AFM topographic images: (a) C18 alkylthiol islands on Au(111) (440 nm × 440 nm), (b) C22 alkylthiol islands on Au(111) (430 nm × 430 nm). Bottom: cursor profiles. In both cases, regions of two different heights are formed, often next to each other. The difference of height between these regions is 5 Å for C18 and 6 Å for C22. Applied load is approximately −20 nN (pull-off force = 30 nN).

3. Results

3.1. AFM Results. For all of the molecules studied we found that three different structural configurations of adsorbed molecules coexist when the coverage is below the full monolayer. Two of them consist of upright molecules with different tilt angles, and the third one consists of flat lying molecules. As determined by AFM, the tilted configurations appear as islands of two different heights. To minimize possible film compression by the tip, the heights of the islands were measured by AFM using the lowest practical point, close to the pull-off force.

The AFM images of Figure 1 show example of islands of C18 (left) and C22 (right) where the two heights are clearly visible. The tallest areas are 18 ± 1 Å for C18 and 21 ± 1 Å for C22. This corresponds to islands with a tilt angle of around 30−35°. These heights are about 4.5 Å lower than expected from the molecular lengths and the 30−35° tilt angle due to a film of flat lying molecules surrounding the islands (see below).[45] The height difference between low and tall configurations is 5 ± 0.5 and 6.0 ± 0.5 Å for C18 and C22, respectively. From these, we infer that for both molecular lengths the chains in the lower height areas are packed with a tilt angle of around 50° away from the surface normal.[42]

To investigate the molecular order, small-size scans were taken to obtain high-resolution images. The lattice periodicity of Au(111) (Figure 2a), obtained by using forces sufficiently high to displace the flat lying molecules, is used as a reference for the accurate determination of size and orientation of the lattices of alkanethiol islands located on the same terrace. For the long molecules (C22 and C18), a $(\sqrt{3}\times\sqrt{3})$R30° structure was resolved on the tall island regions (Figure 2b). On the lower regions, however, a rectangular structure was observed with

(43) Barrena, E.; Ocal, C.; Salmeron, M. *J. Chem. Phys.* **1999**, *111*, 9797−9802.
(44) Kolbe, W. F.; Ogletree, D. F.; Salmeron, M. *Ultramicroscopy* **1992**, *42*−*44*, 1113−1117.
(45) Chain lengths ($L_{C22} = 31.4$ Å, $L_{C18} = 26.4$ Å, and $L_{C10} = 16.4$ Å) are calculated assuming bond angles of 110°, for both Au−S−C and C−C−C, and bond lengths of 2.21 Å (Au−S), 1.81 Å (S−C), 1.54 Å (C−C), and 1.5 Å for the methyl group.

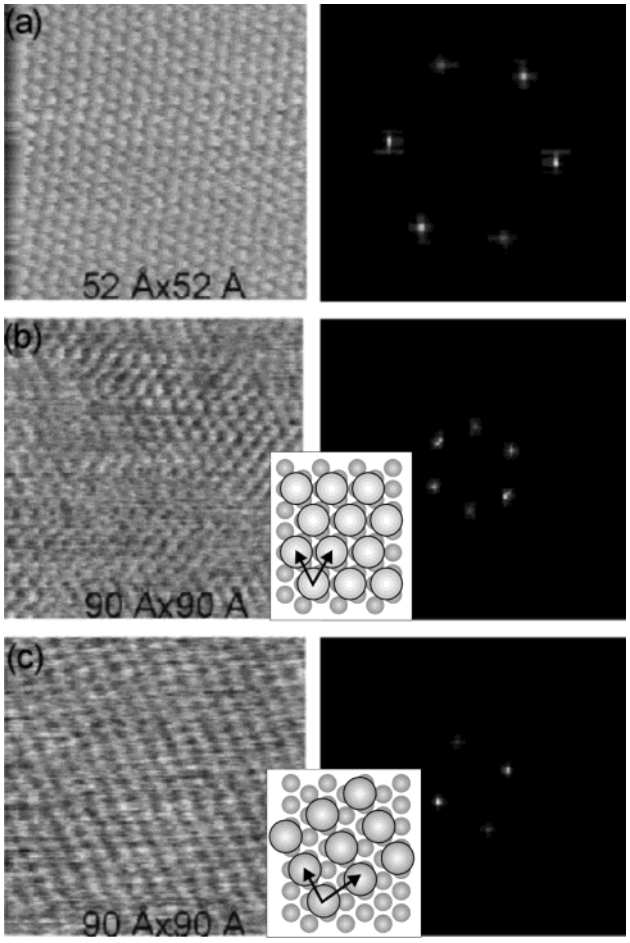

Figure 2. (a) Lattice-resolved image of Au(111) on the terrace between C18 islands. (b) Lattice resolution image showing the $(\sqrt{3}\times\sqrt{3})$R30° structure on top of the taller regions. (c) Lattice resolution image showing the $(2\times\sqrt{3})$rect structure on top of lower regions. Right: 2D-Fourier transformed images. (Small distortion in some of the lattices is due to artifacts of the scanning, that is, nonlinearity and creep of the piezo-scanner.) Insets: schematic models of each structure.

dimensions of 5.9 ± 0.2 and 4.9 ± 0.2 Å along the nearest-neighbor (NN) and next-nearest-neighbor (NNN) directions of the Au(111), respectively. This corresponds to a $(2\times\sqrt{3})$rect structure, already reported for C18,[42] with unit cell dimensions of 5.76 and 4.99 Å (Figure 2c). Three equivalent domain orientations of this structure were observed in different islands, each island consisting of a single domain.

The films formed by shorter molecules (C10) at coverage below the full monolayer were also found to consist of two differently tilted configurations coexisting with flat lying molecules, as shown in Figure 3. The regions labeled a, b, and c correspond to the two tilted regions and the flat lying molecules, respectively. In this case, the difference in height between tall and low islands (a and b) was 3 ± 0.5 Å, which is again consistent with two configurations with approximately 30−35° and 50° tilt angles. The tall areas (a) exhibit the $(\sqrt{3}\times\sqrt{3})$R30° structure (Figure 3a), whereas the lower regions (b) present a rectangular structure (Figure 3b). As in the case of the $(2\times\sqrt{3})$rect lattice obtained for long molecules, the unit cell is parallel to the NN and NNN directions of the Au(111). Interestingly, we found that it consists of pairs of rows as shown in more detail in Figure 4a. The distance between double rows, that is, the periodicity along the NN direction, is 11.4 ± 0.4 Å,

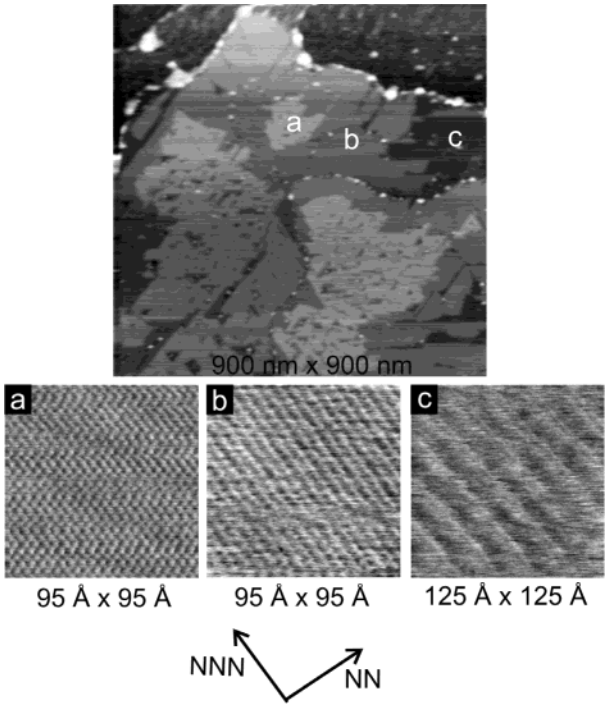

Figure 3. Top: large area AFM topographic image of a C10 partial monolayer showing the coexistence of areas of three different heights, a, b, and c. High-resolution lattice images obtained in each region are shown: (a) hexagonal $(\sqrt{3}\times\sqrt{3})$R30°, (b) rectangular $(4\times\sqrt{3})$rect, and (c) surrounding film of lying-down molecules.

4 times the nearest-neighbor Au(111) distance, while the periodicity along the NNN direction is ∼5 Å, that is, $\sqrt{3}$ times the lattice parameter of Au(111). This corresponds to a $(4\times\sqrt{3})$rect structure. It has the same molecular density as the $(2\times\sqrt{3})$rect (29 Å^2 per molecule) structure, but contains two molecules (1 and 2 in the schematic of Figure 4b) per unit cell. Unfortunately, the internal molecular arrangement cannot be discerned from the images. This is because the AFM topographic images obtained in contact mode provide lattice resolution but no true molecular (atomic) resolution.

By scanning at very low force (as close as possible to the pull-off value), we have also been able to image the structure of the flat lying molecules surrounding the islands. These molecules form ordered stripes, as shown in Figure 3c, running along the NNN direction; that is, they are parallel to the rows of the rectangular structure. The periodicity of the stripes is 20.6 ± 1 Å, very close to the value of 22 Å reported in the literature[15,18,25,26] for the phase denoted as $7.5\times\sqrt{3}$.[46] A more detailed study will be the subject of a forthcoming paper.[47]

3.2. Grazing Incidence X-ray Diffraction Results. To better understand the structure formed by the short chain molecules, GIXD measurements were performed on C10 films deposited on a Au(111) single crystal. The films were prepared in air following the preparation procedure described above for the AFM experiments. The presence of islands with the rectangular structure was checked by AFM prior to introduction into the UHV chamber.

From in-plane diffraction scans (*h* and *k* scans), we could confirm that the unit mesh does indeed correspond to a

(46) This notation describes a striped structure with a periodicity of $\sqrt{3}$ along the stripes and of 7.5 Å between stripes, both multiples of the Au(111) nearest-neighbor distance.
(47) Barrena, E.; Munuera, C.; Salmeron, M.; Ocal, C., to be published.

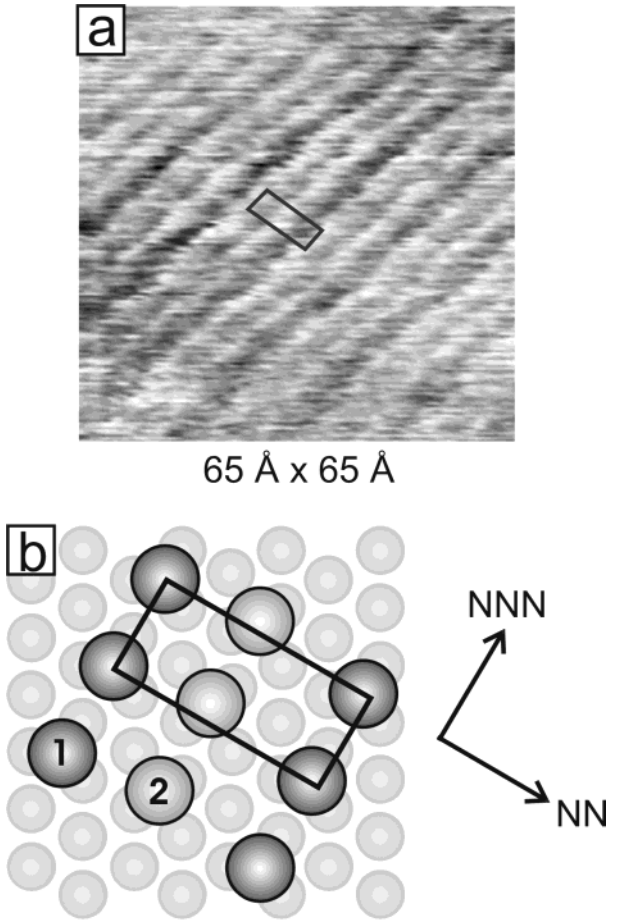

Figure 4. (a) High-resolution image acquired on the top of a C10 island with the 50° configuration. A pair of rows is observed running along the next-nearest-neighbor (NNN) direction of the Au(111). The periodicity perpendicular to the rows (NN direction of the Au(111)) is 11.4 Å, 4 times the Au(111) lattice parameter. A periodicity of 5 Å is observed along the rows. (b) Proposed $(4\times\sqrt{3})$rect model with two nonequivalent molecules (1 and 2). The exact arrangement of the molecules in the unit cell is not known, and therefore other nonequivalent adsorption sites are possible.

$(4\times\sqrt{3})$rect lattice, as shown by the reciprocal space map shown in Figure 5a. Large circles denote the surface diffraction peaks of the Au(111), and small circles correspond to peaks of the rectangular lattice. For simplicity, only one domain is shown. Figure 5b, c, and d shows in-plane rocking scans of the (0,1), (1,0), and (1,1) Bragg peaks of the $(4\times\sqrt{3})$rect structure. At the simplest level, the peak full width at half-maximum (fwhm) or ΔQ of the scans gives a lower limit of the average domain size. Using the relation $\Delta L = 2\pi/\Delta Q$, we obtain from peak (1,1) an average domain size of $L \approx 986$ Å. This is in agreement with the AFM data, which reveal that single domain areas larger than 1000 Å are formed (as seen in Figure 3). The formation of large islands of the hexagonal configuration (mean diameter >1500 Å) has been also observed.[43,48] These large domain sizes indicate that it is easier to obtain larger ordered areas for islands than for complete condensed monolayers.[2,3,28] We believe this result is due to kinetics of the self-assembly process.

The finite size of the islands added to the molecular mobility[43] makes it easier for the molecules to adopt the packing existing around the nucleation sites, and thus islands grow as single domains. For complete monolayers, a large number of nucleation sites combined with limited mobility results in a juxtaposition of different orientations with smaller domain sizes. Full coverage requires annealing to promote coarsening of the domain boundary networks and ripening of gold vacancies for the formation of domains as large as 800 Å.[2,3,28,49]

(48) GIXD experiments performed on the samples of islands confirmed the formation of larger domains than in monolayers whose size was comparable to the average islands size measured by AFM. Unpublished results.

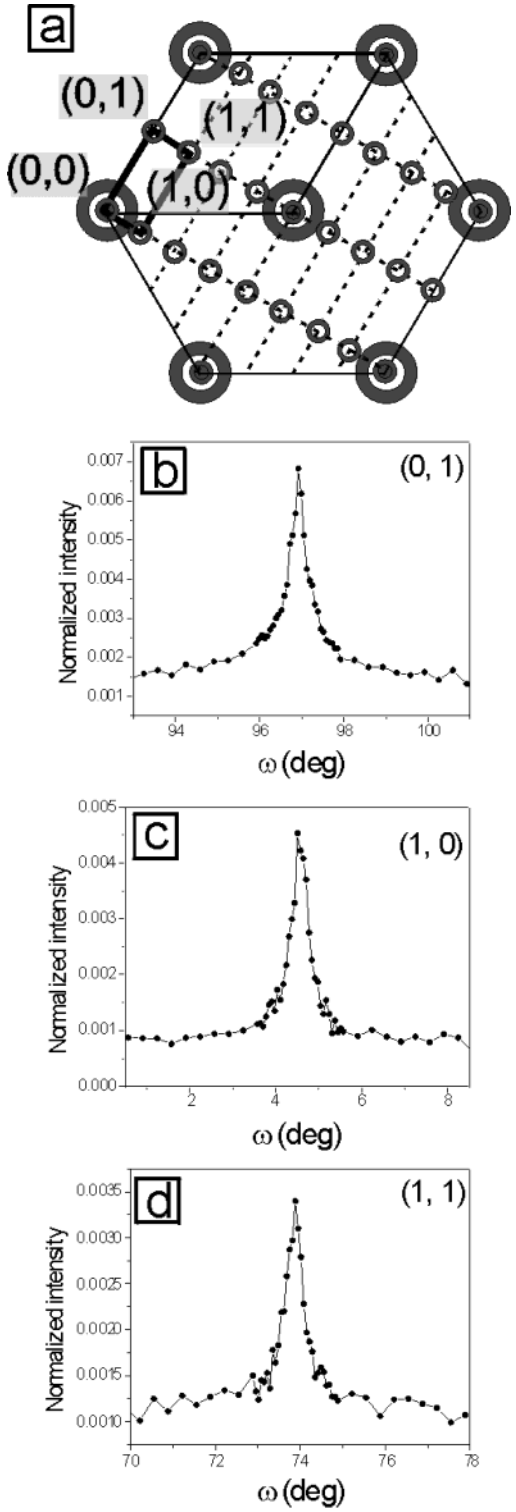

Figure 5. (a) Schematic diagram of the $(4\times\sqrt{3})$rect reciprocal space obtained by GIXD for C10 islands on Au(111). Large circles represent diffraction peaks from the Au(111) substrate. Small circles are due to the rectangular lattice. (b), (c), and (d) show in-plane rocking scans of the (0,1), (1,0), and (1,1) Bragg peaks of the $(4\times\sqrt{3})$rect structure.

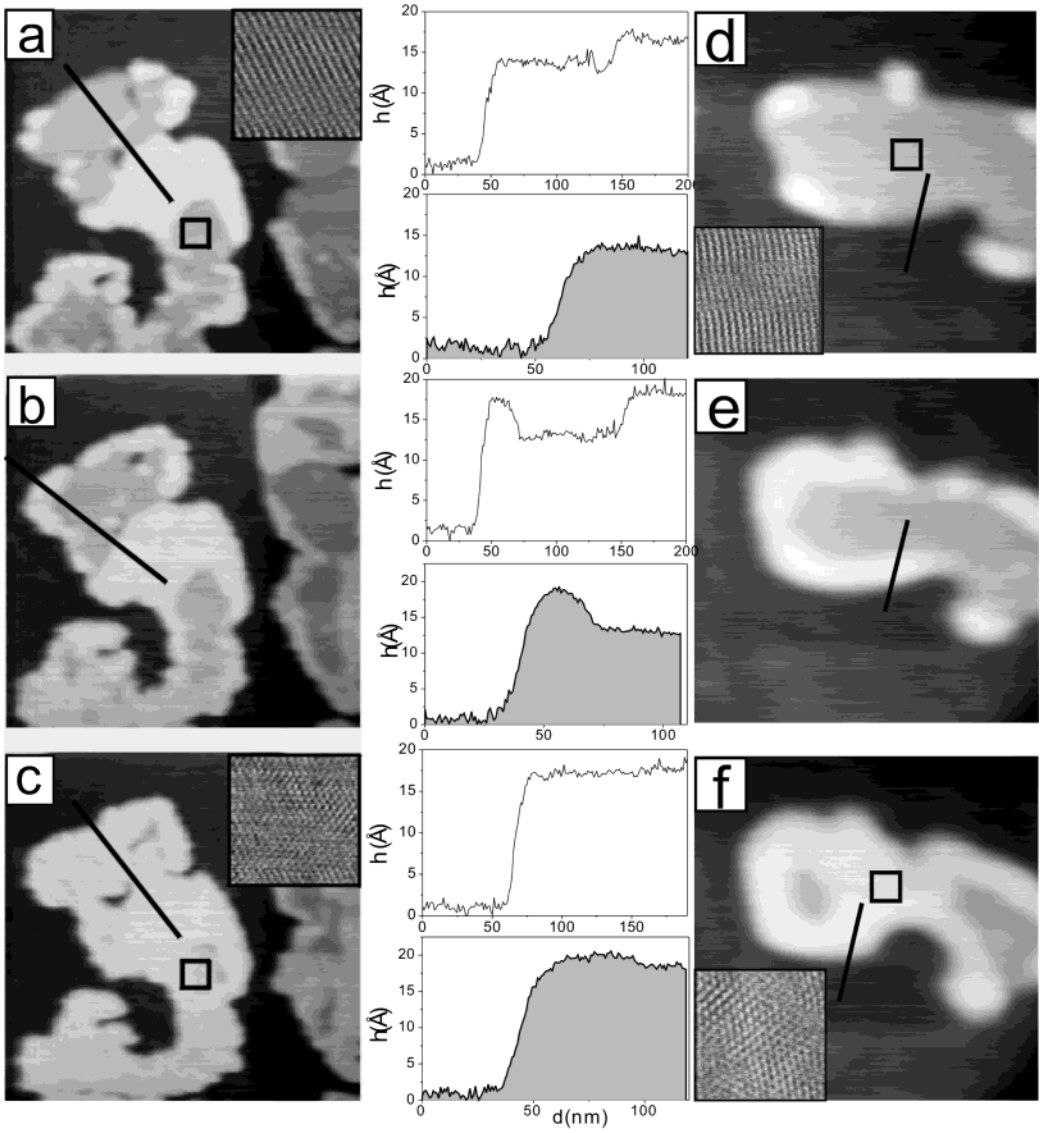

Figure 6. AFM topographic images acquired at a load of $L = 0$ nN showing C18 islands (left) (350 nm × 350 nm) and C22 islands (right) (290 nm × 290 nm). (a) and (d) High (bright) and low (grey) regions with hexagonal ($\sqrt{3}\times\sqrt{3}$)R30° and rectangular ($2\times\sqrt{3}$)rect structures formed spontaneously during film growth and observed at a load (0 nN) below a threshold value which transforms the rectangular structure to the hexagonal structure. (b, e) Images obtained after scanning slightly above the critical load ($L = 12$ nN for C18, $L = 20$ nN for C22). The bright rim surrounding the ($2\times\sqrt{3}$)rect islands has grown in size, indicating the transformation starts near the island edges. (c, f) Images taken after scanning at higher load ($L = 13$ nN for C18, $L = 30$ nN for C22). The tip strongly perturbs the islands, and the molecules rearrange into the more stable ($\sqrt{3}\times\sqrt{3}$)R30° structure. The transformation is nearly complete. Insets: High-resolution images of (15 nm × 15 nm) and (12 nm × 12 nm) for C18 and C22, respectively. Middle column: line profiles (filled area curves correspond to C22 and unfilled curves to C18) showing the height changes.

Unfortunately, due to film damage during prolonged X-ray measurements, it was not possible to measure a large enough set of in-plane structure factors to attempt a crystallographic analysis. Despite this, the present data allow us to discard any model with symmetry not compatible with the GIXD data. The AFM and GIXD results are thus consistent with a ($4\times\sqrt{3}$)rect structure like the one presented in Figure 4b. A possible reason for the nonequivalence between molecules 1 and 2 could be a difference in the adsorption site. This, however, is not yet proven by the measurements.

3.3. Thermal and Mechanical Stability. We now address the question of the thermal and mechanical stability of the newly found 50° tilted configurations of C10, C18, and C22. To test the thermal stability, samples containing islands of C18 with the 50° tilted configuration were annealed at temperatures of 40, 50, 65, 75, and 90 °C. After each thermal treatment, the samples were cooled to room temperature and examined by AFM to check for any possible structural change within the film. The rectangular structure was still observed after annealing up to 75 °C for 30 min. Higher temperatures, however, led to the thermal desorption of the molecules.

In a second set of experiments, the mechanical stability of the 50° tilted configuration was investigated by studying the effect of increasing the load applied by the AFM tip. The experiments were realized in the following way: (i) an area containing the rectangular configuration (50° tilt) was initially imaged at low load; (ii) the same area was then scanned at a higher load; and (iii) the possible induced changes are monitored by reimaging at the initial low load. The procedure is repeated several times at increasingly higher loads.

(49) Camillone, A., III; Leung, T. Y. B.; Scoles, G. *Surf. Sci.* **1997**, *373*, 333−349.

Figure 6 depicts the result of such experiments for C18 (left) and C22 (right). Only the images obtained at step (iii), that is, taken at low force, are shown. Because both molecules were found to behave similarly, only numerical data for C22 are given in the following description. The image of Figure 6d was acquired after scanning at 0 nN and shows a large island with the center part consisting of molecules with 50° tilted configuration. Part of the surrounding region, near the edges, is made of molecules in the 30−35° tilted configuration (brighter in the images). The area was subsequently scanned, increasing the load by steps of 1 nN.

After this, a new image was acquired at the initial low load to monitor possible induced changes in the film. Up to 15 nN, no appreciable changes were observed. However, after scanning at 20 nN, regions near the rim acquired a height equal to that in the tall regions (Figure 6e). After the force was further increased to 30 nN, most of the island exhibits a uniform height of 21 Å (Figure 6f). High-resolution images reveal that the molecules in the low regions, initially with a $(2\times\sqrt{3})$rect structure, were now ordered in the $(\sqrt{3}\times\sqrt{3})$R30° structure. The height changes are illustrated by the topographic profiles in the same figure. Although a region containing both packing structures has been chosen to make these changes more visible, the transition occurs also in isolated $(2\times\sqrt{3})$rect islands, independently of the tip used.

Remarkably, once the transition has been induced, the initial rectangular structure is not recovered either with time or by further manipulation; that is, the transition is irreversible. The transition requires the presence of defects, and thus it starts at the island periphery (Figure 6b). The threshold pressure necessary to induce the transition is similar for both molecular lengths, but varies depending on the degree of compactness of the islands. From our tip radius of 20 nm (estimated by imaging a high aspect ratio conical feature of a calibration sample), we estimate a threshold pressure of about 1 GPa. Film compactness increases after several days from the initial preparation time due to the slow healing of defects inside the islands by a ripening process.[43] This time can be substantially shortened by moderate annealing (to 40 °C during 30 min). In the annealed islands, the threshold pressure required to induce the transition is 1.5−2 times higher.

The same experiment was performed with islands of C10 molecules in the 50° tilted configuration. The results differ completely from those described above for long molecules: no transition to the hexagonal structure occurs. Figure 7 presents a typical example, with 7a and 7b corresponding to the initial images at a load of ∼8 nN showing the $(4\times\sqrt{3})$rect periodicity. After increasing the load to ∼16 nN followed by reimaging at low load, we obtained the images in 7c and 7d. The islands retain their original height and shape. However, structural changes have occurred that are revealed by high-resolution images. These images reveal that, while the rectangular $(4\times\sqrt{3})$rect periodicity is maintained, the molecules have rearranged into another domain of the same rectangular structure but rotated by 60°. As for long molecules, there is a threshold pressure which causes the rupture of the molecular cohesion of the 50° titled configuration. This rupture is followed by a molecular reorganization after the pressure is released that for long chains produces the hexagonal (30° tilted) structure, whereas for the short C10 molecules it produces a differently oriented domain of the same 50° tilted structure. This indicates that the configuration with a tilt angle of 50° in the short C10 chains is more stable than the similarly tilted structure in the longer chains. We shall discuss this point in detail in the next section.

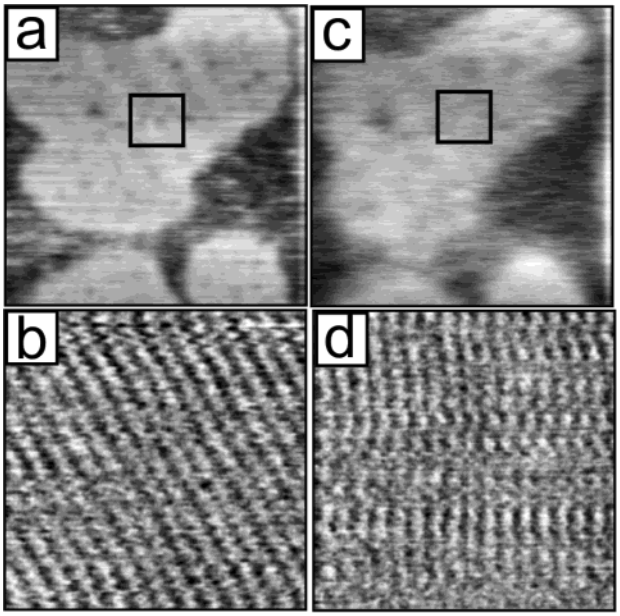

Figure 7. (a) AFM topographic image (225 nm × 225 nm) showing C10 islands in the 50° tilted configuration. (b) Molecular resolution on top of an island after scanning at 8 nN and decreasing the load back to a value close to the pull-off. The image size is 95 Å × 95 Å. (c) and (d) are images of the same area as in (a) and (b), taken after scanning at 16 nN and again decreasing back to near the pull-off. The molecules have rearranged into another rotational domain of the same rectangular structure. No transition to the hexagonal structure is observed. The overall island shape and height are not changed.

4. Discussion

4.1. Molecular Structure and Packing. The equilibrium structure of the adsorbed alkanethiol molecules is the result of the energetic balance between their interaction with the substrate and with the rest of the molecules. On one hand, the strong covalent interaction of the S headgroup with the substrate favors the formation of commensurate structures with the gold lattice. On the other hand, the attractive van der Waals interaction drives the self-assembly and leads to the formation of a dense packing that minimizes the intermolecular distance. The most effective packing is achieved for chains standing upright and with a separation close to their van der Waals diameter ($d \approx 4.3$ Å). Because of the internal structure of the alkane chains, favorable packing is obtained for specific angles dictated by the interlocking of the C−C backbone zigzag.[50−52] A simple geometrical model was used in previous work to calculate the possible tilted configurations observed either under tip compression[53,54] or spontaneous formation.[42] Taking into account the interlocking of one chain with the neighboring molecules, the tilt from the

(50) Kitaigorodskii, A. *Organic Chemical Crystallography*; Consultants Bureau: New York, 1961.
(51) Outka, D. A.; Stöhr, J.; Rabe, J. P.; Swalen, J. D.; Rotermund, H. H. *Phys. Rev. Lett.* **1987**, *59*, 1321−1324.
(52) Ulman, A.; Eilers, J. E.; Tillman, N. *Langmuir* **1989**, *5*, 1147−1152.
(53) Barrena, E.; Kopta, S.; Ogletree, D. F.; Charych, D. H.; Salmeron, M. *Phy. Rev. Lett.* **1999**, *82*, 2880−2883.
(54) Barrena, E.; Ocal, C.; Salmeron, M. *J. Chem. Phys.* **2000**, *113*, 2413−2418.

surface normal (θ) can be described by two angles in two perpendicular directions, θ_x and θ_y, where x runs along the nearest-neighbor molecular direction and y runs along the next-nearest-neighbor direction. The angles at which the chains interlock satisfy the equations

$$\tan(\theta_x) = n \cdot a/d_x \qquad (n = 0, 0.5, 1, 1.5,...)$$

$$\tan(\theta_y) = m \cdot a/d_y \qquad (m/2 = 0, 0.5, 1, 1.5,...)$$

where a corresponds to the distance between alternating carbons along the alkane chain (2.5 Å), d_x corresponds to the distance between molecular planes in the NN direction, and d_y corresponds to twice the distance between molecular planes in the NNN direction. Only some of the structures corresponding to these angles are also commensurate with the substrate.

All tilted configurations observed so far can be satisfactorily explained with our simple geometrical model. The $(\sqrt{3}\times\sqrt{3})$R30° structure is obtained for $n = 0$ and $m/2 = 1$ leading to a tilt of around 35° along the molecular NNN direction. As can be deduced from the previous analysis of the two rectangular structures, no difference in packing density exists within this simple model. Both the $(2\times\sqrt{3})$rect and the $(4\times\sqrt{3})$rect structures are ascribed to configurations with $\theta_x = 41°$ and $\theta_y = 30°$ ($n = 1$, $m/2 = 1.5$), which leads to a total tilt angle of 50°.[42] Therefore, the intermolecular van der Waals interactions contribute similarly to the total energy in the two configurations. In the energy estimations discussed below, they will be considered as the same structure.

Among the possible configurations satisfying the angular relationships shown above, only the commensurate structures are spontaneously formed. The noncommensurate structures are only obtained under tip compression and disappear after the load is released.[53,54] This shows that the stability of any configuration is not only determined by van der Waals interactions between chains but also by S−Au interfacial interactions, which control the formation of structures commensurate with the Au(111) lattice.

For all three chain lengths studied, the commensurate 50° tilted configurations were seen to spontaneously form from solution, indicating that they are stable versus thermal energy excitations ($kT = 26$ meV at room temperature). This suggests that the formation of such phases is a rather general phenomena in alkanethiols at coverage intermediate between the striped phases and the $c(4 \times 2)$ monolayer.

Similar to what was reported in gas-phase deposition studies,[21,23,25] we observe that several phases of different molecular density coexist. For our sample preparation procedure (very dilute solutions, ambient conditions,...), where kinetic effects and out of equilibrium growth can play an important role, these phases are as follows: the close-packed structure (30° tilted), the rectangular (50° tilted) configuration, and a lying-down phase.

Large tilt angles have been observed for alkanethiols on GaAs,[55] but no evidence of a 50° phase was found in UHV studies from gas-phase deposition of alkanethiols on gold. However, an STM study on C12 monolayers formed by microcontact printing has reported the formation of a $(4\times\sqrt{3})$rect low-density structure when very low concentrations of ink (micromolar) were employed.[56] Although the STM images do not provide information about film height (and therefore tilt angle), it is likely that this structure is similar to the 50° tilted configuration reported here. Some of the structures reported at intermediate coverage, whose periodicity differs from that of the striped phases, might correspond as well to tilted structures.[32−34,38]

Apart from the role of the interactions contributing to self-assembly (see below), some experimental factors, as a slow adsorption process induced by the use of very dilute solutions and short immersion times or the presence of water during molecular reorganization, cannot be disregarded concerning the formation of the 50° tilted configuration.

4.2. Mechanism of Transition between the 50° and 30° Configurations. In section 3.3, we have described a series of experiments illustrating the consequences of increasing the compressive stress exerted by the AFM tip over films ordered in the 50° molecular packing for both short and long molecules. The possible changes in the structure or morphology were monitored after the compressive stress was released. When the experiment was performed on C18 or C22 islands (exhibiting the 50° tilted configuration), the film reorganized into the 30° structure only after the pressure was above a certain threshold value.

This phenomenon can be understood as a rupture of the cohesive packing at the threshold pressure followed by molecular "reassembling" after the pressure is released: when the applied pressure is above a certain value (threshold value), the energy is sufficient to damage the molecular packing of the islands via creation of vacancies, removal of molecules, etc. When the load is released, fast diffusion processes driven by the van der Waals interaction between molecules lead to the reassembling of the island in a time-scale lower than the scanning time (seconds).[57] As we have seen, the long molecules reassemble in the hexagonal configuration, while short molecules reassemble in a rectangular configuration, usually with a different orientation but energetically equivalent.

The fact that for C18 and C22 the 50° tilted structure transforms irreversibly to the hexagonal configuration when mechanically excited by the tip indicates that it is metastable. Although the threshold load for the transformation varies from sample to sample (depending on island compactness), we can estimate the energy dissipated in the process by evaluating the work done by the tip. During compression at the threshold load L_{thr}, the tip moves by Δh toward the surface (reduction of film height) and by $\Delta h \times \tan 20°$ in the horizontal direction (due to the tilted ~20° mounting of the cantilever). The work performed is then $W = (L_{thr} + L_{adh}) \times \Delta h + F_{fric} \times \Delta h \times \tan 20°$. L_{adh} is the adhesion force, and F_{fric} is the friction force at this load. The second term is much smaller than the first, due to the small value of F_{fric}, typically 10 times smaller than L_{thr}.[53] For C18 islands, L_{thr} is close to 26 nN, $\Delta h = 3$ Å, and $L_{adh} = 3$ nN. The energy per molecule is then obtained by dividing this energy by the number of molecules under the tip at the threshold load. For our tip radius (20 nm) and using the elastic properties of

(55) Sheen, C. W.; Shi, J.-X.; Märtenson, J.; Parikh, A. N.; Allara, D. L. *J. Am. Chem. Soc.* **1992**, *114*, 1514−1515.

(56) Larsen, N. B.; Biebuyck, H.; Delamarche, E.; Michel, B. *J. Am. Chem. Soc.* **1997**, *119*, 3017−3026.

(57) When the applied pressure is very high, the island breaks apart in debris which are displaced away by the tip. In this case, the molecular rearrangement can take place in a scale of hours or days.[43]

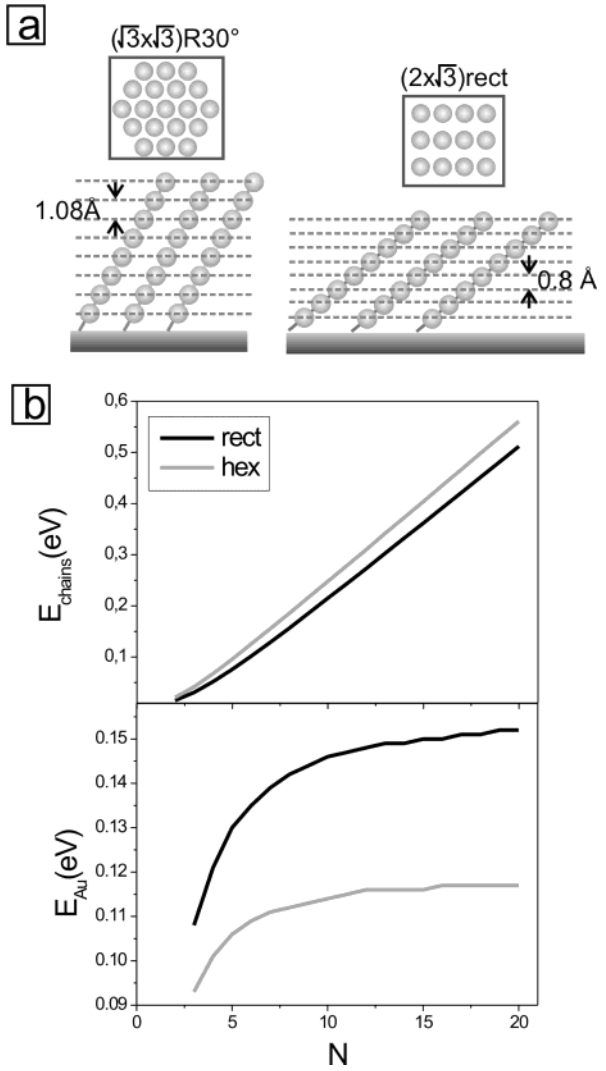

Figure 8. (a) Model used to calculate van der Waals energies in the $(\sqrt{3}\times\sqrt{3})$R30° and $(2\times\sqrt{3})$rect tilted configurations. (b) Top graphs: cohesive energy per molecule, calculated for each packing, assuming additive van der Waals interactions between the CH_2 of all of the chains. The more tilted (50°) configuration has a lower cohesive energy and is energetically less favorable than the hexagonal packing when only this interaction is considered. Bottom graphs: energy per molecule due to the interaction with the substrate (using a modified Lennard-Jones potential). This term favors the formation of the rectangular packing because the molecule is closer to the substrate.

alkyl chains within a simple Hertzian contact model, we obtain 0.4 eV per molecule.[58] This is of the order of magnitude of the cohesive energy of the chain packing and is therefore sufficient to cause the separation of the close-packed molecules. It is also sufficient to induce changes in the adsorption site of the sulfur atoms at the interface (the corrugation energy of the Au(111) surface is 0.26 eV[59,60]).

The different behavior observed for long and short molecules needs, however, further explanation. We have thus estimated the difference in energy between the 50° tilted and the 30° stable configurations as a function of the chain length.

4.3. van der Waals Modeling. To understand the relative stability of the tilted configurations as the molecular length varies, we performed calculations based on a simple model. In this model, the alkane chains are represented by a linear array of spherical methylene units that lie in planes parallel to the gold substrate, as shown in Figure 8a. In the hexagonal configuration, the CH_2 groups are ordered in a hexagonal structure with a lattice parameter of 4.99 Å within each plane. We assume a tilt angle of 30° and neglect any small variation that might exist as a function of chain length.[41] Because the distance between methylene units is 1.25 Å (projection of the C−C bond along the chain axis), the planes are separated by $1.25\cdot\cos 30° = 1.08$ Å. Similarly, the 50° tilted rectangular configurations are described in terms of planes separated 0.88 Å with the CH_2 groups ordered in a 5.76 Å × 4.99 Å lattice within each plane. As discussed in the previous section, this describes both the $(2\times\sqrt{3})$rect and the $(4\times\sqrt{3})$rect structures.

The interactions to be considered are the following: (i) between chains, (ii) between chains and gold substrate, and (iii) covalent interaction between sulfur and the Au(111) surface. Although of crucial importance for the assembling process, we can assume that the third term does not depend on the chain length and therefore will not be considered in the calculation where only differences in energy are relevant.

For the intermolecular interactions, we use pure van der Waals forces. Assuming additivity, the cohesive energy per molecule is calculated by summing A/r^6 pair potentials between units of one chain and the rest of the film. The constant A is adjusted such that the computed total energy for a C18 chain equals the heat of sublimation for the corresponding saturated alkane molecules, which is 1.3 eV/molecule.[61] Assuming a compact hexagonal packing of C18 alkanes with an average separation between chains of 4.3 Å (the approximate van der Waals diameter[50]), a value for A equal to 26 eV Å^6 is obtained.

The sum has been performed in the following way. We consider the CH_2 group at position i along one chain and sum the A/r^6 terms corresponding to all of the CH_2 units situated in a plane located k methylene units away from i (it is sufficient to limit the summation to the first 100 neighbors). The contribution from all planes is then added to obtain E_i. Finally, the cohesive energy per molecule is calculated by summing over all of the CH_2 groups of the chain:

$$E_{\text{chains}}(N) = \sum_{i=0}^{N-1} E_i$$

N is the number of carbons in the chain.[62] We consider the energy as positive for attractive potentials; that is, the higher the energy is, the more stable the structure is. The total van der Waals energy per molecule obtained in both configurations, hexagonal and rectangular, is represented in the top graph of Figure 8b. It shows that the cohesive energy due to packing is always smaller for the 50° tilted configuration (rectangular). This can be intuitively understood on the basis of pure geometric arguments: although the separation between molecules is the same in both configurations, the methylene groups located near the end of the chains have fewer nearest neighbors for the more tilted chains.

(58) By using $E_{Si3N4} = 140$ Gpa (Young's modulus), $\nu_{Si3N4} = 0.2$ (Poisson's ratio), $E_{SAM} = 9.3$ Gpa, $\nu_{SAM} = 0.4$, we obtained a contact radius of 3.5 nm. Assuming a defect-free rectangular molecules packing (i.e., 29 Å^2 per molecule), approximately 132 molecules are under the tip.
(59) Sellers, H.; Ulman, A.; Shnidman, Y.; Eilers, J. *J. Am. Chem. Soc.* **1993**, *115*, 9389−9401.
(60) Yourdshahyan, Y.; Zhang, H. K.; Rappe, A. M. *Phys. Rev. B* **2001**, *63*, 081405(R)-1−4.
(61) Israelachvili, J. *Intermolecular and Surface Forces*; Academic Press: San Diego, CA, 1991; p 89.
(62) Salmeron, M. *Tribol. Lett.* **2001**, *10*, 69−79.

We consider now the interaction of each CH_2 group with the Au(111), which is also of van der Waals type. The value of A should now be higher because one of the interacting bodies is a metal (high polarizability). The force will be stronger the closer the methylene unit is to the gold surface, that is, the larger the tilt angle. This interaction between CH_2 groups and the gold will be described by the Lennard-Jones potential of Hautman and Klein,[63] where the attractive term has been integrated over the substrate (a half-space). The resulting interaction of one CH_2 group with the Au(111) surface is

$$U(z)_{\mathrm{Au}} = \frac{-2413}{(z-0.86)^{12}} + \frac{1.47}{(z-0.86)^{3}}$$

Again, we use the convention of attractive forces giving positive energies. We assume that the distance between the carbon closest to the S and the gold surface is the same for both configurations. The Au−S−C and the C−C−C angles are taken as 110°, and the bond lengths are taken as Au−S = 2.21 Å,[64] S−C = 1.81 Å,[50] and C−Au = 3.28 Å. The energy per molecule (E_{Au}) has been calculated for both configurations by summing over the N methylene groups of the chain to obtain

$$E_{\mathrm{Au}}(N) = \sum_{i=0}^{N-1}\left[\frac{-2413}{(i{*}1.25{\cdot}\cos\theta + 3.28 - 0.86)^{12}} + \frac{1.47}{(i{*}1.25{\cdot}\cos\theta + 3.28 - 0.86)^{3}}\right]$$

where θ is the tilt angle (30° or 50°). The results are presented in Figure 8b (bottom graph). The energy increases with the chain length, but saturates at approximately $N = 9$ for the hexagonal and $N = 12$ for rectangular structures. Not surprisingly, the more tilted configurations are favored.

The total energy can then be calculated for each structure by adding the two terms. The difference of total energy between the hexagonal and the rectangular configurations is represented in Figure 9b as a function of the number of carbons in the chains:

$$\Delta E(\mathrm{N}) = E_{\mathrm{hex}}(\mathrm{N}) - E_{\mathrm{rect}}(\mathrm{N})$$

For films of molecules with more than nine carbons, the difference in energy is positive, indicating that the hexagonal configuration is energetically more favorable. For the shorter chain lengths, the attractive interaction with the substrate turns out to be more important than that between chains, and the energy difference between both structures decreases, until finally it becomes negative for molecules with less than nine carbons. This indicates that the rectangular structure becomes more stable for these shorter chains.

We are aware that by using such a simple model, quantitative calculations cannot be provided. A more refined model should be implemented including the structure of the backbone, the molecular orientation, and the sulfur−gold interface.

Despite its simplicity, this calculation allows us to understand the experimental results and clearly illustrates the role played by the different interactions in the energetic balance determining the structure. For long molecules (C18 and C22), the van der Waals interaction between chains plays the dominant role, and the hexagonal structure is the most stable configuration even at partial coverage. The metastable 50° tilted configuration corresponds to a local minimum in the energy (Figure 9a) and forms most likely as a result of favorable kinetic pathways. Once formed, an activation barrier has to be overcome to transform into the most stable configuration. The observed existence of a metastable configuration indicates that this energy barrier is higher than the available thermal excitation energy. When higher energy excitations are imposed on the system, like the perturbation by the AFM tip, the molecules reorganize into the more stable hexagonal configuration.

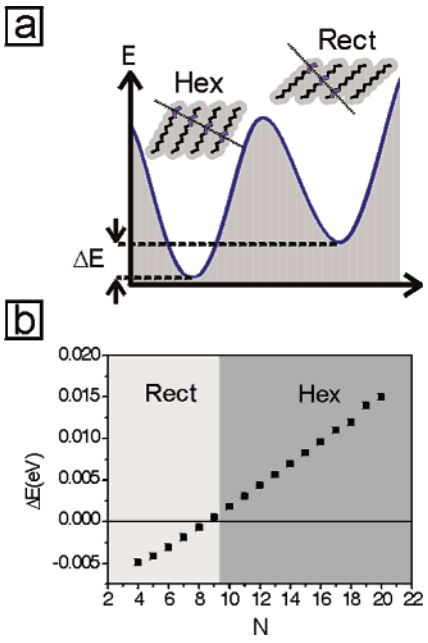

Figure 9. (a) Qualitative schematics energy diagram for the hexagonal (30°) and the rectangular (50° tilt) structures. (b) Calculated energy difference between the hexagonal and rectangular configurations as a function of the chain length, $\Delta E(\mathrm{N}) = E_{\mathrm{hex}}(\mathrm{N}) - E_{\mathrm{rect}}(\mathrm{N})$. For chains with less than nine methylene units, the rectangular configuration is energetically favored.

5. Conclusions

The present study shows for first time the formation of ordered 50° tilted configurations at intermediate coverage (between that of the striped phase and the close-packed monolayer) for molecules of different chain lengths, C10, C18, and C22. The tilt angle and periodicity of the structures have been unambiguously determined by AFM and supported by GIXD experiments that provided an accurate determination of the molecular lattice.

At coverage under a full monolayer, alkanethiols spontaneously self-assemble into two types of upright but tilted configurations: a hexagonal $(\sqrt{3}\times\sqrt{3})$R30° structure characteristic of the monolayer, with the alkyl chains tilted 30−35° from the vertical, and a rectangular $(2\times\sqrt{3})$rect structure with a molecular tilt of 50°. For short molecules (C10), a $(4\times\sqrt{3})$rect structure with similar tilt angle and molecular density is formed. Islands exhibiting the hexagonal and the rectangular structures coexist with a phase of flat lying molecules.

The stability of the 50° tilted configuration varies as a function of the chain length. Long molecules (C18, C22) initially in the rectangular 50° tilted configuration transform into the

(63) Hautman, J.; Klein, M. L. *J. Chem. Phys.* **1989**, *91*, 4994−5001.
(64) Fenter, P.; Schreiber, F.; Berman, L.; Scoles, G.; Eisenberger, P.; Bedzyk, M. J. *Surf. Sci.* **1998**, *412/413*, 213−235.

($\sqrt{3}\times\sqrt{3}$)R30° structure (30° tilted) after mechanical perturbation by the AFM tip that can deliver energy, substantially above thermal energy fluctuations at room temperature, to promote the rupture of molecular cohesion. In contrast, short molecules reassemble again in the rectangular 50° tilted structures after the same manipulation. This evidences a higher stability of the rectangular structure for the shorter chain lengths.

We have estimated the difference in energy between the 30° and 50° tilted configurations by considering the competition between intermolecular and molecule−substrate interactions. The calculation indicates that, whereas the cohesive energy of the chain packing diminishes for large tilt angles, the energy due to the interaction with the substrate increases, with the balance between the two contributions depending on chain length. The intermolecular van der Waals interaction dominates for long molecules, and the close-packed ($\sqrt{3}\times\sqrt{3}$)R30° structure is the most stable. For short molecules (around 10 carbons long), the interaction with the substrate turns out to be an equally important contribution that favors the stability of the 50° tilted phase.

Acknowledgment. This work has been supported by the Comunidad Autónoma de Madrid under Grant No. 07N/0025/2001 and by the Director, Office of Energy Research, Office of Basic Energy Sciences, Material Science Division, of the U.S. Department of Energy under Contract No. DE-AC03-76F00098. The GIXRD measurements were performed during SI-714 beam time at the ESRF. C. Munuera thanks the Spanish MEC for a predoctoral scholarship. Verona Maus is acknowledged for support in the thiol synthesis. U. Jonas would like to thank Prof. H. W. Spiess for his continued support.

JA036143D